Published OnlineFirst November 12, 2018; DOI: 10.1158/1078-0432.CCR-18-0936

Translational Cancer Mechanisms and Therapy

Clinical Cancer Research

Preclinical Efficacy of Endoglin-Targeting Antibody–Drug Conjugates for the Treatment of Ewing Sarcoma

Pilar Puerto-Camacho[1], Ana Teresa Amaral[1], Salah-Eddine Lamhamedi-Cherradi[2], Brian A. Menegaz[2], Helena Castillo-Ecija[3], José Luis Ordóñez[1], Saioa Domínguez[4], Carmen Jordan-Perez[1], Juan Diaz-Martin[1], Laura Romero-Pérez[1], Maria Lopez-Alvarez[1], Gema Civantos-Jubera[1], María José Robles-Frías[1], Michele Biscuola[1], Cristina Ferrer[4], Jaume Mora[3], Branko Cuglievan[2], Keri Schadler[2], Oliver Seifert[5], Roland Kontermann[5], Klaus Pfizenmaier[5], Laureano Simón[4], Myriam Fabre[4], Ángel M. Carcaboso[3], Joseph A. Ludwig[2], and Enrique de Álava[1]

Abstract

Purpose: Endoglin (ENG; CD105) is a coreceptor of the TGFβ family that is highly expressed in proliferating endothelial cells. Often coopted by cancer cells, ENG can lead to neoangiogenesis and vasculogenic mimicry in aggressive malignancies. It exists both as a transmembrane cell surface protein, where it primarily interacts with TGFβ, and as a soluble matricellular protein (sENG) when cleaved by matrix metalloproteinase 14 (MMP14). High ENG expression has been associated with poor prognosis in Ewing sarcoma, an aggressive bone cancer that primarily occurs in adolescents and young adults. However, the therapeutic value of ENG targeting has not been fully explored in this disease.

Experimental Design: We characterized the expression pattern of transmembrane ENG, sENG, and MMP14 in preclinical and clinical samples. Subsequently, the antineoplastic potential of two novel ENG-targeting monoclonal antibody–drug conjugates (ADC), OMTX503 and OMTX703, which differed only by their drug payload (nigrin-b A chain and cytolysin, respectively), was assessed in cell lines and preclinical animal models of Ewing sarcoma.

Results: Both ADCs suppressed cell proliferation in proportion to the endogenous levels of ENG observed *in vitro*. Moreover, the ADCs significantly delayed tumor growth in Ewing sarcoma cell line–derived xenografts and patient-derived xenografts in a dose-dependent manner.

Conclusions: Taken together, these studies demonstrate potent preclinical activity of first-in-class anti-ENG ADCs as a nascent strategy to eradicate Ewing sarcoma.

Introduction

Ewing sarcoma is the second most common primary bone and soft tissue sarcoma of children, adolescents, and young adults. It results from pathognomonic balanced t(11;22)(q24;q12) chromosomal translocations between *EWSR1* and one of several genes in the ETS family of transcription factors. Micrometastatic spread is nearly universal at the time of diagnosis, and about one-quarter of patients with Ewing sarcoma present with radiologically-evident metastatic disease at that time.

Although the long-term survival rate has improved over the last few decades for those who present with localized disease, mainly due to the introduction of multimodal therapeutic strategies, the 5-year survival rate in patients with metastatic disease remains below 20%–30% (1). Poor clinical outcomes can, in part, be attributed to tumor cell heterogeneity and varied expression of the fusion-protein expression (2), which influences the epigenomic (3, 4), transcriptomic, and proteomic profiles (5) of the cells. Ultimately, those changes regulate cell phenotype and drug sensitivity (3, 6).

This implies a critical need to shift from an outdated 'one fits all' therapeutic approach to a more customized treatment strategy directed towards the unique molecular traits that exist within each tumor. Toward that end, ADCs have been used with increasing frequency in the last few decades as a precision-guided treatment to combat cancer and are now an essential weapon in the oncologists' arsenal of antineoplastic therapies (7). ADCs consist of an mAb joined to a cytotoxic agent by a chemical linker. Among a wide range of cytotoxic molecules, we evaluated the type-2

[1]Institute of Biomedicine of Sevilla (IBiS), Virgen del Rocio University Hospital/CSIC/University of Sevilla/CIBERONC, Seville, Spain. [2]Department of Sarcoma Medical Oncology, MD Anderson Cancer Center, Houston, Texas. [3]Institut de Recerca Sant Joan de Déu, Pediatric Hematology and Oncology, Hospital Sant Joan de Déu Barcelona, Spain. [4]Oncomatryx, Derio, Bilbao, Spain. [5]IZI, University of Stuttgart, Germany.

Note: Supplementary data for this article are available at Clinical Cancer Research Online (http://clincancerres.aacrjournals.org/).

P. Puerto-Camacho, A.T. Amaral, and S.-E. Lamhamedi-Cherradi contributed equally to this article.

J.A. Ludwig and E. de Álava are senior corresponding authors.

Corresponding Authors: Enrique de Álava, Instituto de Biomedicina de Sevilla (IBiS), CSIC-Universidad de Sevilla, Avda. Manuel Siurot, s/n., Sevilla E-41013, Spain. Phone: 34-955013029; Fax: 34-955013029; E-mail: enrique.alava.sspa@juntadeandalucia.es; and Joseph A. Ludwig, Department of Sarcoma Medical Oncology, MD Anderson Cancer Center, 1901 East Road, Building 4SCBR2.1042, Houston, TX 77054. jaludwig@mdanderson.org

doi: 10.1158/1078-0432.CCR-18-0936

Published OnlineFirst November 12, 2018; DOI: 10.1158/1078-0432.CCR-18-0936

Translational Relevance

Antibody–drug conjugates represent an innovative therapeutic strategy with growing interest in the clinic. Endoglin is a mesenchymal stem cell marker, which plays an important role in the TGFβ pathway. In this study, we demonstrate for the first time that anti-endoglin drug conjugates are a promising option for the treatment of Ewing sarcoma. Herein, we show that the expression of endoglin in Ewing sarcoma cell lines, patient-derived xenograft models, and tumor samples is heterogeneous. Hence, the screening of endoglin expression in tumor samples as a predictive marker of response to anti-endoglin antibody–drug conjugates represents a crucial step. Treatment with anti-endoglin antibody–drug conjugates, using two different drug payloads, nigrin-b A chain and cytolysin, in cell line-derived xenografts and patient-derived xenograft models, led to a drastic tumor reduction. These findings provide a strong rationale for the implementation of anti-endoglin antibody–drug conjugates in the context of precision medicine in Ewing sarcoma.

ribosome-inactivating protein nigrin-b A chain and the microtubule-disrupting synthetic small molecule cytolysin (8, 9). Irrespective of the type of cytotoxic payload fused to the mAb, the targeting antibody recognizes tumor tissues by specifically binding to the cognate cell surface protein. Once the ADC is internalized via receptor-mediated endocytosis, the drug is released into the late endosome compartment and becomes active (7, 10). The mechanism of action of ADCs can be incredibly specific, and off-target effects can often be limited to tissues that selectively express the target of interest (10).

ENG is a homodimeric glycoprotein that acts as a coreceptor of TGFβ family of proteins. It occurs in two isoforms and exists at the tumor cell surface and tumor microenvironment within the extracellular matrix (11). ENG is also expressed in endothelial cells (EC), activated macrophages, normal marrow cells, some leukemic cells, and other types of tumor cells. Transmembrane ENG usually exists as part of a multiprotein complex that can include TGFβ receptor 1 (ALK1, ALK5), TGFβ receptor 2, and BMP receptors (12, 13). Soluble ENG (sENG), however, is predominantly distributed in the extracellular matrix (ECM) following cleavage by MMP14 (14). Its expression plays a key role during embryogenesis, angiogenesis, vascular development and homeostasis (15, 16). Of particular relevance to our work, ENG is highly expressed by a range of human sarcomas and by human mesenchymal stem cells (MSC), the putative Ewing sarcoma cell of origin (17). Notably, its expression has been linked to cell plasticity, an especially-important finding given that Ewing sarcoma is a poorly differentiated neoplasm with no normal tissue counterpart. Further, the sentinel trait of Ewing sarcoma plasticity and epigenetic dysregulation appears to facilitate vasculogenic mimicry and promote tumor cell invasiveness (18–20).

Herein, we sought to better understand how ENG contributes to Ewing sarcoma biology while teasing apart the direct and indirect contribution of ENG-targeting. Critically, with an eye towards a future clinical development, our research leverages the strength of two independent laboratories to validate the preclinical results. Independently, we establish that human-specific anti-ENG ADCs are superior to unconjugated ENG-targeting therapies in their capacity to suppress cell proliferation and hinder tumor growth. Furthermore, we demonstrate a number of heretofore unreported tumor-centric effects that have a major impact on critical cell signaling pathways. Although naked anti-ENG MAbs (e.g., TRC105) are already being tested across a diverse window of tumor types, our data suggest that ADCs could significantly improve the likelihood of clinical benefit.

Materials and Methods

Cell lines and cell cultures

A4573, CADO, ES8, RDES, RM82, TC32, VH64, and TC71 ES cell lines were cultured in complete RPMI medium. Other Ewing sarcoma cell lines, A673 and SKNMC, were cultured in DMEM 4.5 g/L glucose and EMEM medium, respectively. All the cell culture media were supplemented with 1% penicillin/streptomycin, 1% glutamine, and 10% FBS (all from Gibco, Thermo Fisher). All parental cell lines were tested twice per year for mycoplasma contamination using the MycoAlert Detection Kit (Lonza Group Ltd.) according to the manufacturer's protocol and authenticated using either short tandem repeats (STR) fingerprinting with an AmpFLSTR Identifier Kit as previously described or STR analysis (CLS, Cell Lines Service GmbH). Cell line individual characteristics and origin are depicted in Supplementary Table S1. All commercially available cell lines were purchased from ATCC, and each were used for no longer than 3 months.

Patient studies

Plasmas from patients with Ewing sarcoma ($n = 27$) were kindly provided by Dr. Arjan Lankester from the Leiden University Medical Center. Patient samples, (plasma, tumor) were obtained under patient consent and in accordance to Declaration of Helsinki. Plasmas from healthy donors ($n = 7$) were obtained under patient consent by the Centro de Investigación del Cáncer in Salamanca, Spain. A cohort of 22 Ewing sarcoma samples embedded in Tissue-Tek O.C.T. compound (Sakura Finetek USA Inc.) and an additional cohort of 43 FFPE samples [used to generate tissue microarray (TMA)] were obtained from the Hospital Universitario Virgen del Rocío-Instituto de Biomedicina de Sevilla Biobank (Andalusian Public Health System Biobank and ISCIII-Red de Biobancos PT13/0010/0056). All identified patients and collected data were in accordance with guidelines of MDACC and IBIS's institutional review board. Authors followed the recommendations suggested by REMARK guidelines.

Animal experiments

All experiments were conducted in accordance with protocols and conditions approved by the European guidelines (EU Directive 2010/63/EU) and by the University of Texas MDACC (Houston, Texas) Institutional Animal Care and Committee (eACUF Protocol #00000928-RN01). *In vivo* binding assay, dose-ranging–study and RM82 xenograft models were approved by the local institution and the Dirección General de la producción Agrícola y ganadera de la Junta de Andalucía in Spain. PDX studies were approved by the local animal care and use committee (Comité Ético de Experimentación Animal at Universidad de Barcelona, protocol 419/15). ES8 xenograft model was approved by the University of Texas MD Anderson Cancer Center Institutional Animal Care and Use Committee (ACUF Protocol#000928-

Published OnlineFirst November 12, 2018; DOI: 10.1158/1078-0432.CCR-18-0936

RN01). Additional material and methods are provided in the Supplementary Information section.

Results

ENG is heterogeneously expressed in Ewing sarcoma cell lines and PDX models

ENG expression was evaluated in a set of Ewing sarcoma cell lines, using MSCs and an endothelial cell line (HUVEC) as positive controls. The Ewing sarcoma panel comprises cell lines bearing various EWS–ETS fusion variants (Supplementary Table S1). *ENG* mRNA and protein levels varied considerably across the Ewing sarcoma cell lines (Fig. 1A and B). The CADO cell line lacked expression of *ENG*, both at the mRNA (Fig. 1A), and at the protein levels (Fig. 1B). This heterogeneous expression of ENG prompted us to analyze the methylation status of the CpG islands present in *ENG* promoter in Ewing sarcoma cell lines. In fact, the *ENG* promoter was only hypermethylated in the CADO cell line, suggesting that ENG expression is epigenetically regulated in Ewing sarcoma (Fig. 1C; Supplementary Fig. S1A). In addition, compared with CADO cell line, the ENG was expressed in RM82 (high level) and TC71 (intermediate-low level) cell lines, as

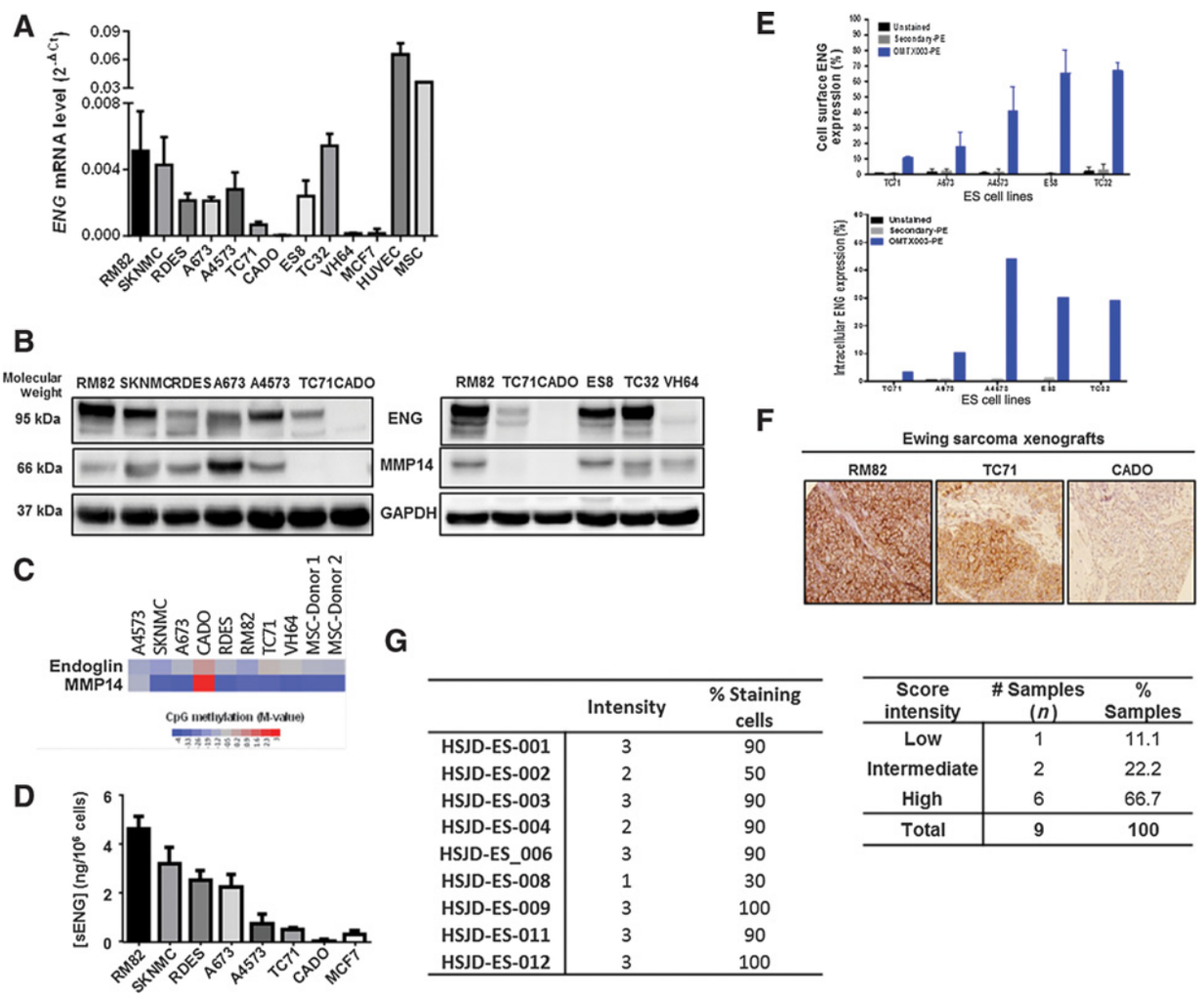

	Intensity	% Staining cells
HSJD-ES-001	3	90
HSJD-ES-002	2	50
HSJD-ES-003	3	90
HSJD-ES-004	2	90
HSJD-ES_006	3	90
HSJD-ES-008	1	30
HSJD-ES-009	3	100
HSJD-ES-011	3	90
HSJD-ES-012	3	100

Score intensity	# Samples (*n*)	% Samples
Low	1	11.1
Intermediate	2	22.2
High	6	66.7
Total	9	100

Figure 1.

Heterogeneous expression of ENG/MMP14 in Ewing sarcoma (ES) cell lines and xenografts. **A** and **B,** The expression of ENG was heterogeneous among ES cell lines at both mRNA (**A**) and protein (**B**) levels measured, respectively by qRT-PCR and Western blotting ($n = 10$). **B,** Similarly, heterogeneous expression of MMP14 was observed at the protein level as determined by Western blot analysis ($n = 10$). **C,** The methylation status of *ENG/MMP14* genes in the CADO cell line suggests that these genes are regulated at the epigenetic level (GSE#118872). **D,** The soluble form of ENG was detected at the extracellular compartment by ELISA in a set of ES cell lines ($n = 7$) that express ENG. MCF7 cells are used as a negative control. **E,** Cell surface and intracellular expression of endoglin as assessed by flow cytometry against a panel of human ES cells. The OMTX003 vehicle antibody exhibits linear dose-dependent binding and effectively discriminates between medium-low–expressing (TC71 and A673) and high-expressing (ES8, TC32, and A4573) cell lines. **F,** Maintained expression of ENG was confirmed in RM82, TC71, and CADO xenograft tumors of ES ($n = 3$), respectively with high, intermediate-low, and negative expression. **G,** Heterogeneous expression of ENG was investigated in nine PDX models of ES, which are screened based on the intensity of stain and percentage of stained cells. The frequency of ENG expression intensity (high, intermediate, or low) was presented on the right table.

confirmed by immunofluorescence (Supplementary Fig. S1B) and FACS analyses (Supplementary Fig. S1C). When cleaved by MMP14, ENG is shed into the extracellular matrix in a soluble form (sENG), which can also be detected in the supernatants of Ewing sarcoma cell lines ($n = 7$) by ELISA (Fig. 1D). Here, sENG concentration positively correlated with the mRNA levels of ENG (Pearson's correlation: $r = 0.7747$, $P = 0.0408$; Supplementary Fig. S1D). sENG was also evaluated in human plasma from healthy donors and patients with Ewing sarcoma; however, no significant differences were observed between healthy donors/Ewing sarcoma-patient, localized/metastatic disease, or low/high tumor volume groups (Supplementary Fig. S2A–S2C). Finally, no link between sENG and clinical parameters was observed (Supplementary Fig. S2F). One possible explanation for this finding could be that the constitutive concentration of sENG in the organism may be overlapping the differential tumor-derived sENG concentration, as ENG is expressed in physiologic conditions.

In parallel, ENG expression was characterized by flow cytometry analysis in a panel of five Ewing sarcoma cell lines (ES8, TC32, TC71, A4573, and A673) using the OMTX003 vehicle antibody at their cellular membrane and intracellular levels. OMTX003 exhibited linear dose-dependent binding and effectively discriminated between low-expressing (TC71 and A673) and high-expressing (ES8, TC32, and A4573) cell lines (Fig. 1E). ENG expression was also evaluated by IHC analysis in a set of Ewing sarcoma xenograft ($n = 3$, Fig. 1F) and PDX models ($n = 9$, Fig. 1G), altogether confirmed heterogeneous expression of ENG. In the group of PDX tumors, this heterogeneous ENG expression was also confirmed ranging from 11.1% low, 22.2% intermediate to 66.7% high levels (Fig. 1G).

MMP14 expression positively correlates with ENG expression in Ewing sarcoma cell lines and patients

We investigated the expression of MMP14 within a panel of Ewing sarcoma cell lines (Fig. 1B; Fig. 2A and B) and determined whether this could be useful as a prognostic factor. The CADO cell line, which exhibited no ENG expression (Fig. 1B; Fig. 2B), showed a lack of MMP14 expression and hypermethylation of its promoter (Fig. 1C; Supplementary Fig. S1A). To clarify if MMP14 is the metalloprotease implicated in the extracellular domain cleavage of ENG in Ewing sarcoma, we could not find any correlation between *MMP14* and *ENG* at their mRNA expression levels ($r = 0.6053$; $P = 0.1498$ by Pearson's-Supplementary Fig. S2D); however, we observed a positive correlation between the mRNA levels of *MMP14* and the concentration of sENG in Ewing sarcoma cell line supernatants ($n = 5$; $r = 0.9531$; $P = 0.0121$ by Pearson's-Supplementary Fig. S2E). Furthermore, frozen tissue samples from one cohort of patients with Ewing sarcoma ($n = 22$) were used to evaluate the mRNA expression of *ENG* and *MMP14* (Fig. 2C) and FFPE tissues from another cohort ($n = 43$) of patients were used to evaluate protein expression of ENG and MMP14 (Fig. 2D; Supplementary Table S3) by IHC. High ENG expression was found in 51.16% of the analyzed samples (Fig. 2F). In both cohorts, we found a significant correlation between ENG and MMP14 at their mRNA and protein levels ($r = 0.8331$, $P < 0.0001$, Fig. 2E; and $r = 0.4614$, $P = 0.0021$, Fig. 2D, respectively). These results were in agreement with the *in vitro* data in Ewing sarcoma cell lines and PDX models, demonstrating heterogeneous expression of *ENG* and *MMP14* in Ewing sarcoma samples. The pattern of ENG and MMP14 protein expression did not correlate with the clinical parameters either in the presence of primary, metastatic, or relapse tumors.

ADCs impair *in vitro* Ewing sarcoma cellular proliferation in an ENG expression–dependent manner

Having shown that ENG is highly expressed not only in the endothelium, but also variably-expressed in tumor cells, we sought to isolate the relative contribution of targeting ENG within the vascular stroma versus tumor. As a nontumoral *in vitro* cell-based assay for OMTX003 drug efficacy, HUVEC cells were exposed to this antibody. It was shown previously that OMTX003 binds to human ENG extracellular domain (amino acids 26-584) in a concentration-dependent manner, with high specificity and affinity (Supplementary Fig. S3C). Incubation of OMTX003 with human rhENG or human HT1080 cells showed OD_{50} at 0.3 and MFI_{50} at 0.4 nmol/L by ELISA and flow cytometry analyses, respectively (Supplementary Fig. S3C and S3D).

Incubation of OMTX003 (100 μg/mL, 699.3 nmol/L) with HUVEC cells for 72 hours was able to inhibit tube formation (Supplementary Fig. S4B). ES cell lines presenting the ability to form vasculogenic mimicry (Supplementary Fig. S4A) were also exposed to OMTX003 within the same conditions (Supplementary Fig. S4C), however no effects were observed. Because ENG has been reported to enhance Ewing sarcoma cell proliferation, we assumed that the maximal antiproliferative effect of OMTX003 would occur in Ewing sarcoma cells that abundantly express ENG. To test that hypothesis, three Ewing sarcoma cell lines with varied ENG expression were chosen for experimental validation: RM82 (high expression), TC71 (medium-low expression), and CADO (no expression) cell lines. Surprisingly, we observed little to no effect of OMTX003 in these cell lines (Fig. 3A). Although OMTX003 was able to achieve more than 50% suppression in the ENG-high expressing RM82 cells, the requirement for micromolar range drug concentrations suggested that ENG targeting using naked MAbs such as OMTX003 may not adequately impair Ewing sarcoma cell proliferation.

Considering the promise of ADC technology, we assessed whether drug conjugation to OMTX003 could enhance its antiproliferative effect in Ewing sarcoma cells. Two ADCs were generated by cystein-based conjugation of OMTX003 to either the ribosome-inactivating protein nigrin-b A chain (OMTX503), using the 4-succynimidyloxycarbonyl-α-methyl-α-(2-pyridyldithio)toluene (SMPT) chemical linker, or the microtubule disrupting cytotoxic drug cytolysin (OMTX703), using the protease-cleavable vcPABA optimized linker (Fig. 3B). Similarly to OMTX003, both ADCs were highly stable and able to bind with high specificity and affinity to human ENG on the surface of ENG-expressing cells and got internalized efficiently to allow specific intracellular release and activation of their payload moieties (data not shown). As anticipated, OMTX503 demonstrated a compelling anti-proliferative effect in the assessed Ewing sarcoma cells: RM82 (high ENG expression; $IC_{50} = 1.18 \times 10^{-10}$ M), TC71 (medium-low ENG expression; $IC_{50} = 9.155 \times 10^{-9}$ M), and CADO cell lines (no ENG expression; $IC_{50} \approx 1.738 \times 10^{-8}$ M; Fig. 3C). As shown in Fig. 3D, the sensitivity of Ewing sarcoma cell lines to this agent positively correlated with ENG expression ($r = -0.9999$; $P = 0.0082$). A parallel evaluation was performed to assess the *in vitro* efficacy of OMTX703 by choosing ES8 cell line, which presents the highest expression of ENG among other Ewing sarcoma cell lines to validate the assay (Fig. 1E). This high expression level of ENG in ES8 correlated with efficient

Published OnlineFirst November 12, 2018; DOI: 10.1158/1078-0432.CCR-18-0936

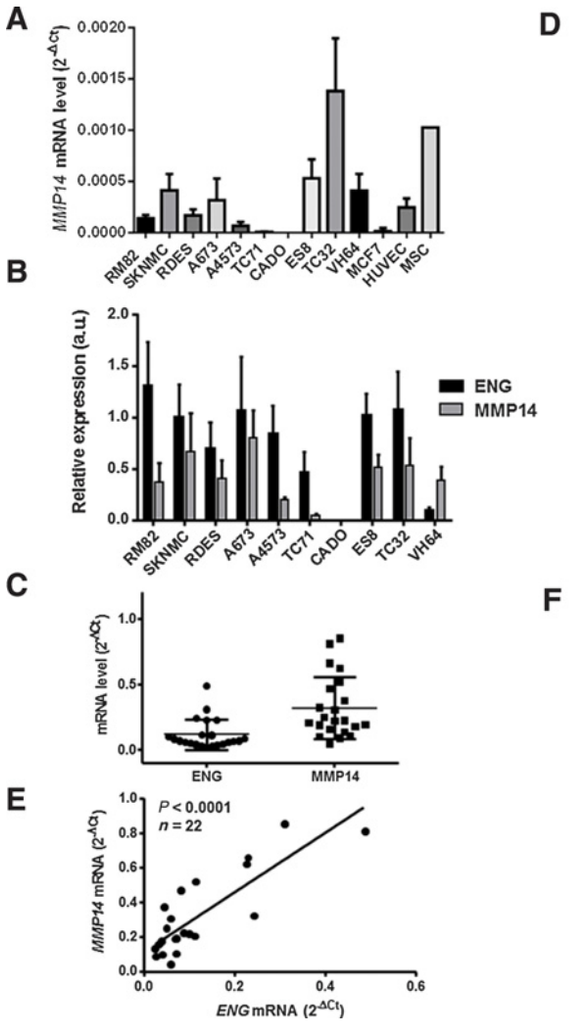

D

	Patients (n = 43)	Samples (n)	Samples (%)
ES patients	Primary	29	67.4
	Metastasis	8	18.6
	Relapse	6	14
	Total	43	100
ENG expression	Low	10	23.26
	Intermediate	11	25.58
	High	22	51.16
	Total	43	100
MMP14 expression	Low	13	30.23
	Intermediate	11	25.58
	High	19	44.19
	Total	43	100

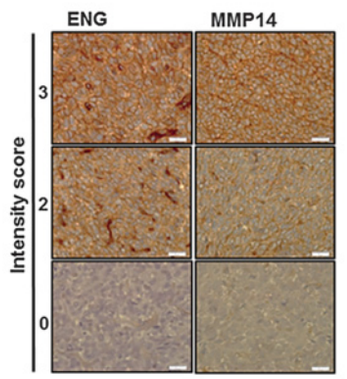

Figure 2.

MMP14 expression correlates with ENG levels in ES cell lines and patients. **A** and **B,** *MMP14* presents a heterogeneous expression among ES cell lines, as determined by qRT-PCR (**A**). Relative protein expression of both ENG/MMP14 after normalization against GAPDH is depicted in (**B**). **C,** Heterogeneous expression of *ENG* and *MMP14* at the mRNA levels measured by qRT-PCR in a cohort of 22 frozen ES tumor samples. **D,** Evaluation of ENG and MMP14 expression by IHC in 43 FFPE ES tumor samples. **E,** Significant correlation between ENG and MMP14 at the mRNA levels ($r = 0.8331$, $P = 0.0001$). **F,** Representative images of different intensity scores (0, 2, 3) of ENG/MMP14 expression in patients with ES.

internalization (data not shown), efficacy, and cytotoxic effects *in vitro* through cell proliferation assays (Fig. 3E, IC_{50} = 260.6 nmol/L). Collectively, these data indicate that ADCs impair *in vitro* Ewing sarcoma cell proliferation in an ENG expression-dependent manner.

ENG-targeting ADCs exhibit on-target effects in Ewing sarcoma animal models

To initiate animal studies, we determined first whether high ENG expression by Ewing sarcoma xenografts (RM82 and CADO) is required to achieve an *in vivo* effect, as our *in vitro* data suggested would be the case. Importantly, as assessed by IHC, the expression of ENG in the xenograft tumors was maintained at levels comparable to the *in vitro* parental cell lines (Fig. 1F). As a second pivotal control, the *in vivo* binding assay confirmed that OMTX003 binds specifically to human ENG, which was only present in tumor cells, but not in the murine-derived microvessels (Fig. 4A). A murine OMTX003 MAb version (OMTX003-mu) targeting ENG was also used to detect its binding to murine-derived vessels expressing ENG, as it was observed in the lower panel of Fig. 4A. To evaluate the adequate therapeutic window of the drugs, a dose-ranging study (DRS) was performed. OMTX003 (unconjugated MAb) and OMTX503 (nigrin-b A chain-ADC) were tested *in vivo* in dose-escalated manner and the animal weight loss (defined as a loss >20% of the initial animal weight) was assessed as an indirect metric of general drug toxicity (Fig. 4B). The vehicle OMTX003 MAb elicited no toxicity when tested at 10 mg/kg in both RM82, CADO (Fig. 4B), and ES8 (Fig. 5A and B) xenograft models. OMTX503 dosing at 0.5 mg/kg also appeared safe. Following euthanasia, careful histopathologic analyses of the lung, liver, and kidney were performed, showing no significant deviation from normality.

Published OnlineFirst November 12, 2018; DOI: 10.1158/1078-0432.CCR-18-0936

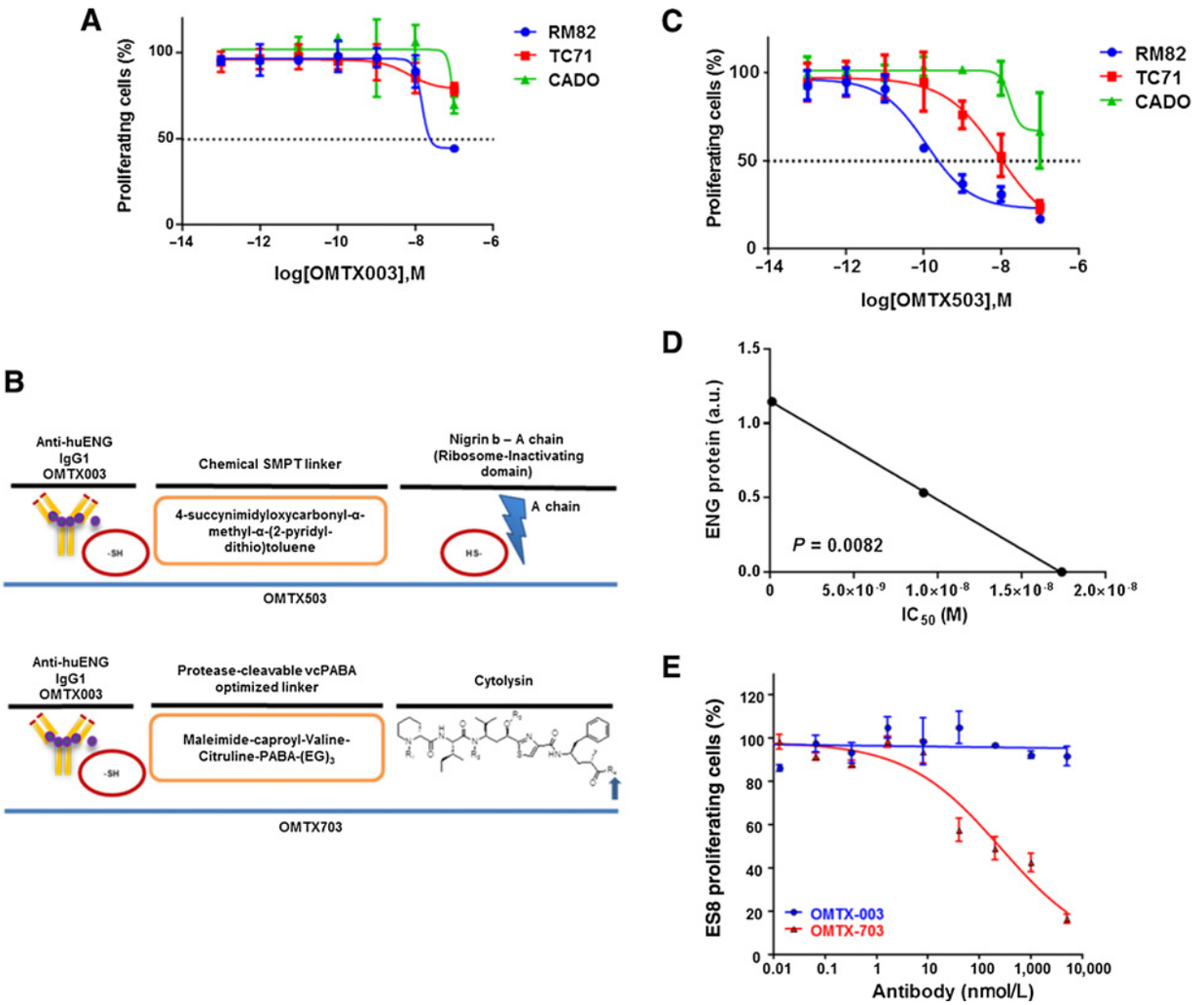

Figure 3.

ES cells are affected *in vitro* by ENG-ADCs treatment within an ENG expression–dependent manner. **A,** OMTX003 was tested on three ES cell lines: RM82, TC71, and CADO, which show differential expression of ENG, in order to evaluate *in vitro* the effect of this ADC on the proliferation rate of these cell lines. **B,** Chemical structure of the OMTX-ADC, ENG MAb candidate lead linked to a cytotoxic agent, nigrin-b A chain (OMTX503) or cytolysin (OMTX703). **C,** OMTX503 activity was tested on these cell lines, which resulted in an inhibition of their proliferation rate in an ENG expression–dependent manner. **D,** There is a significant correlation between the IC_{50} of OMTX503 over the ES cell lines RM82, TC71, and CADO and the ENG protein expression of these cell lines ($r = -0.9999$, $P = 0.0082$). **E,** OMTX003 and OMTX703 were tested during 72 hours in WST1 proliferation cell-based assay using ES8 cell line. Only OMTX703 showed a significant inhibition of ES8 cell proliferation in a dose-dependent manner ($IC_{50} = 260$ nmol/L).

ENG-targeting ADCs impair Ewing sarcoma xenografts tumor growth

The efficacy of OMTX003 and OMT503 was evaluated in RM82 xenografts in parallel with irinotecan (Supplementary Table S4), which was used as a positive control of drug efficacy (Supplementary Fig. S5A). The evolution of tumor growth in each individual group was assessed throughout the 21-day treatment period. The irinotecan-treated group was maintained in a long-term survival study until day 41, when all animals relapsed and were sacrificed (Supplementary Fig. S5A). Animal weight was also evaluated during this time as a measure of treatment-induced toxicity (Supplementary Fig. S5B). Notably, significant delays in tumor growth were observed in OMTX503-treated mice by day 13 ($P = 0.0218$, Fig. 4C), and tumor growth inhibition (TGI) was higher than 50% after 15 days posttreatment (Fig. 4D; Supplementary Table S5). ENG and MMP14 expressions (Supplementary Fig. S5C and S5D) were similar in tumor samples from all groups, as evaluated by IHC (Supplementary Tables S6–S9). H&E staining on the tumor samples revealed a loss of tumor viability in those groups treated with OMTX003 and OMTX503 after day 15 of treatment (Fig. 4E). Systemic signs of toxicity were found in some mice from the OMTX503-treated groups. The macroscopic toxicity observed was not translated into weight loss, as the tumor growth masked the global weight change (Supplementary Fig. S5B). Collectively, these results suggest that the internalization of an immunotoxin by targeting ENG in Ewing sarcoma xenografts impaired tumor growth.

Published OnlineFirst November 12, 2018; DOI: 10.1158/1078-0432.CCR-18-0936

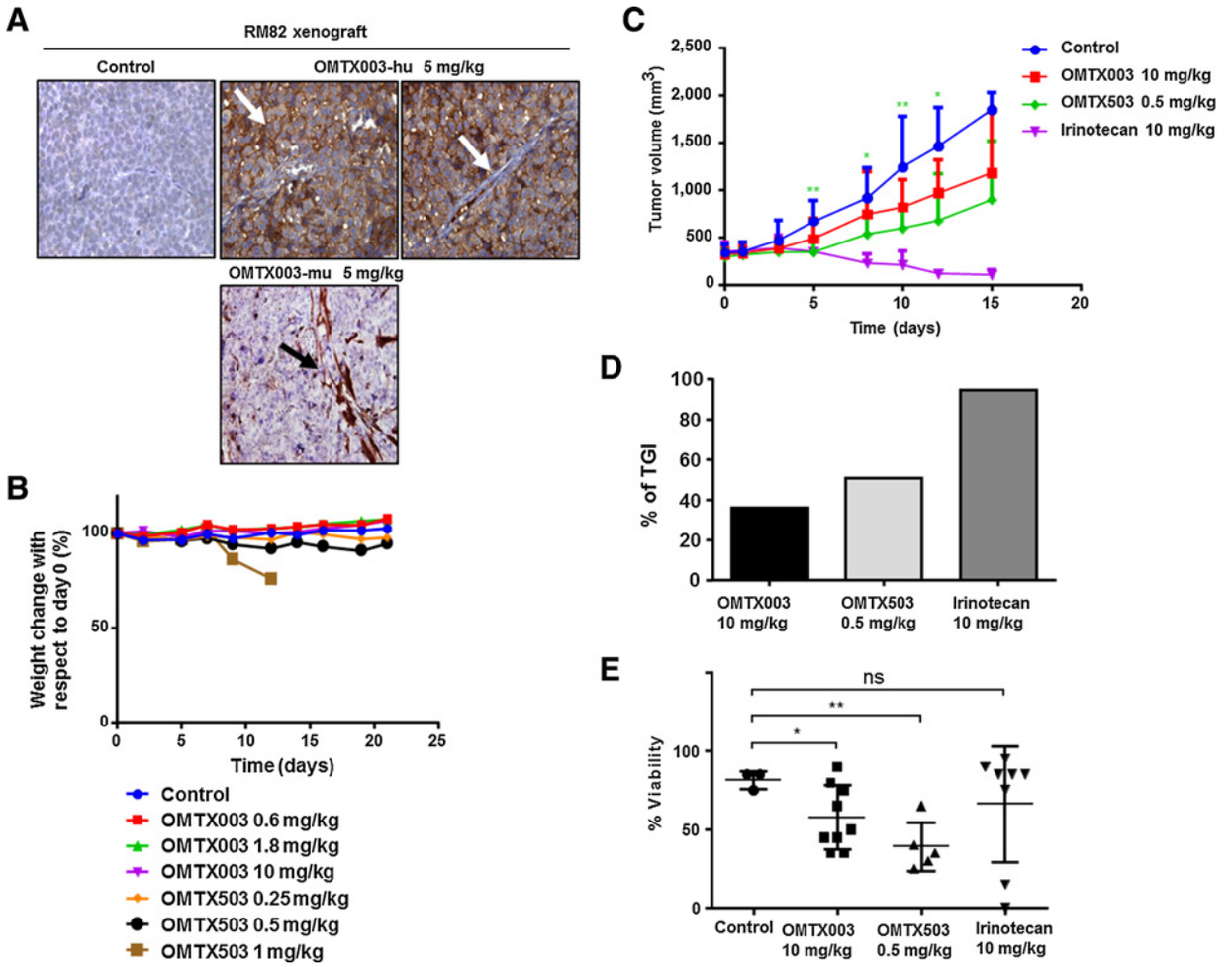

Figure 4.

OMTX503 impairs *in vivo* Ewing sarcoma (ES) tumor growth at a safe concentration. **A,** *In vivo* binding assay: OMTX003 specifically binds to RM82 cell membranes (as indicated with a white arrow in the middle image) but not in murine-derived microvessels within the xenograft tumor (as indicated with a white arrow in the far right image of the panel). In contrast, the murine targeting MAb (OMTX003-mu) binds specifically to the microvessels and is undetected in the membrane of the tumor cells as indicated with a black arrow in the lower image of the panel. **B,** Comparison of normalized body weight during drug treatment in RM82 xenografts ($n = 3$ animals per group). **C** and **D,** Therapeutic effect of OMTX503 in RM82 ES xenografts. Tumor volumes were reported after treatment with OMTX003, OMTX503, PBS as negative control, and irinotecan as positive control ($n = 9$ animals per group). **C,** Curves showing mean tumor volumes for RM82 xenograft tumors during the drug treatments. * represents significance between OMTX503 0.5 mg/kg and the control group: at day 5, $P = 0.0008$; at day 7, $P = 0.0118$; at day 10, $P = 0.0064$; and at day 12, $P = 0.0218$. **D,** Tumor growth inhibition at day 15 in RM82 xenografts treated with OMTX003, OMTX503, and irinotecan ($n = 5$, $n = 7$, and $n = 9$ animals per group, respectively). **E,** Cell viability percentage using H&E stain in different treated RM82 tumors at day 15 with OMTX003 (10 mg/kg, $P = 0.010$) and OMTX503 (0.5 mg/kg, $P = 0.002$). * and ** represent the significance of difference between two groups of treated mice, respectively $P < 0.05$ and $P < 0.005$ according to two tailed, paired Student *t* test.

To test the efficacy of OMTX703 (cytolysin-ADC) in ES8 xenograft, an additional preclinical study was conducted. Tumor growth and Kaplan–Meier curves revealed only modest antitumor activity of OMTX703 at 30 mg/kg, as shown in Fig. 5A–C. Tumor growth was markedly impaired using the highest dose of OMTX703 (60 mg/kg, $P = 0.019$). Having determined an optimal dose for OMTX703, an additional experiment was conducted to assess the mechanism(s) of OMTX703 action and its potential mechanism(s) of resistance following a 2-week exposure to OMTX703 at 0, 10, 30, and 60 mg/kg; 246 proteins were assessed by reverse-phase protein lysate array (RPPA, GSE#114866). ANOVA, Pearson's correlation as distance metric and Ward's linkage as the clustering method using an FDR of 0.01, identified 60 proteins that discriminated between treatment groups. By principal component analysis (PCA), tumor specimens from mice treated with OMTX703 at 10 mg/kg clustered tightly with the placebo-treated group, suggesting that this dose had limited effect (Supplementary Fig. S6C). Surprisingly, two specimens from the OMTX703 group treated at 60 mg/kg nearly overlapped the placebo-treated cluster (Fig. 5D); further scrutiny of these specimens suggested that they had acquired resistance and begun to progress (Supplementary Fig. S6A). RPPA analysis of the xenograft-treated specimens demonstrated two major and five minor clusters. Cluster 1 was associated with proteins significantly downregulated by OMTX703 at 30 and 60 mg/kg compared with a heterogeneously-treated group of tumors from mice that

Published OnlineFirst November 12, 2018; DOI: 10.1158/1078-0432.CCR-18-0936

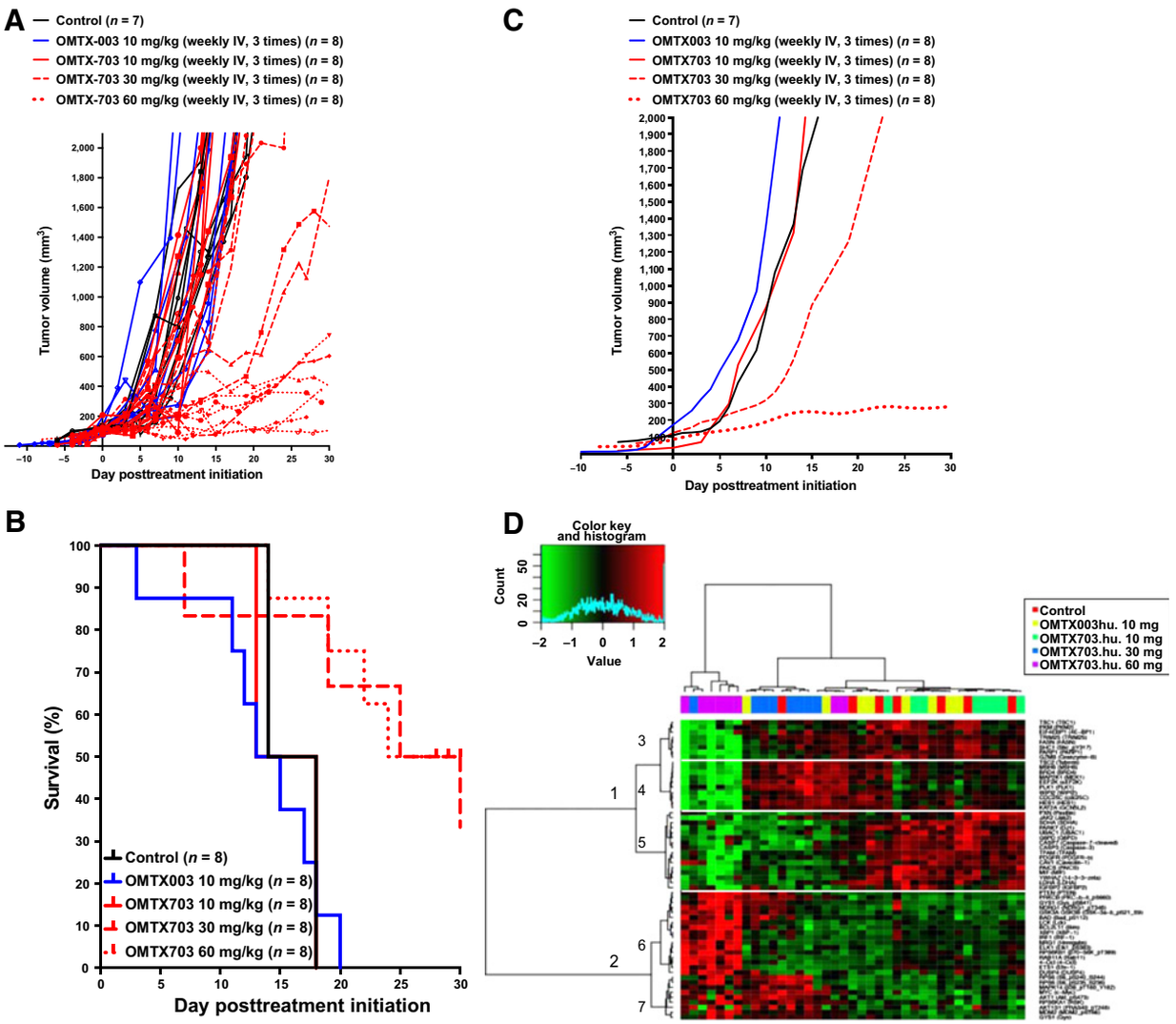

Figure 5.

OMTX703 strongly reduces tumor growth in ES8 xenograft models. **A,** Therapeutic effect of OMTX003 and OMTX703 in ES8 Ewing sarcoma (ES) xenografts. Immunocompromised NOD-SCID-IL-2Rg$^{null/null}$ mice (NSG) were injected with 1×10^6 ES8 cells at their flank. Treatment with OMTX003 ($n = 8$), OMTX703 ($n = 8$, for each dosing group), or control vehicle ($n = 7$) was started when tumor volumes reached of about 100 mm^3. The curves show individual tumor volumes for a period of 30 days of drug exposure. **B,** The panel shows Kaplan–Meier curves. The $P < 0.019$ value for differences between the treated OMTX703 (60 mg/kg) and control mice were performed with the log-rank (Mantel–Cox) test. **C,** The curves show the smoothed grouped median relative tumor volumes. The OMTX703 (60 mg/kg) treatment shows a significant blockade of ES8 tumor growth as compared with control group of mice using unpaired t test and two-tailed P value ($P < 0.0001$). However, no significant effect of low doses OMTX (10 or 30 mg/kg) on this tumor growth. **D,** RPPA profiling (GSE#114866) of control ($n = 7$), OMTX003-treated (10 mg/kg; $n = 8$), OMTX703-treated (10 mg/kg; $n = 8$), OMTX703-treated (30 mg/kg; $n = 8$), and OMTX703-treated (60 mg/kg; $n = 8$) ES8 xenografts following a 2-week exposure identifies statistically significant 60 proteins at a FDR of 0.01.

received placebo control, a naked anti-endoglin Ab (OMTX003), or a subtherapeutic (i.e., 10 mg/kg) dose of the OMTX703 ADC. Gene set enrichment analysis (GSEA) indicated marked suppression of proteins linked to insulin receptor signaling or downstream effectors such as PI3K and mTOR, pathways of known importance in Ewing sarcoma (Supplementary Fig. S7). In contrast, the most differentially upregulated proteins resulting from OMTX703 treatment (cluster 2, Supplementary Fig. S8) were linked to genes associated with nerve growth factor (NGF) and its cognate receptor (TRKA). Obviously GSEA relies upon gene set enrichment and fails to reflect the site-specific protein phosphorylation states that can markedly affect protein function. Thus, the collective effect that individual phospho-proteins have upon pathway activation must be further scrutinized.

To investigate the proteomic changes associated with the heightened clinical activity of the 60 mg/kg dose, a secondary analysis was performed, which grouped the 10 mg/kg OMTX703 samples and the 10 mg/kg OMTX003 ones with the placebo-treated samples (Supplementary Fig. S6B). Using a FDR of 0.0001, an absolute log2-fold change of 1.5, Pearson's correlation as distance metric and Ward's linkage as the clustering method, 22 proteins were discriminately identified between the

Published OnlineFirst November 12, 2018; DOI: 10.1158/1078-0432.CCR-18-0936

three treatment groups (Supplementary Fig. S6B). Notably, a protein regulator of altered metabolism (RPS6) was exclusively upregulated following OMTX703 (60 mg/kg), and a second metabolism biomarker (LDHA) was downexpressed in the 30 and 60 mg/kg-treated groups.

Efficacy study of ENG-targeting ADCs in PDX models of Ewing sarcoma

Finally, we evaluated the efficacy of OMTX703 by using a PDX model that many believe predicts drug activity better than cell lines. Considering the *in vitro* data that indicate ENG expression is required to elicit an antiproliferative effect, an initial Ewing sarcoma PDX panel was screened to identify a suitable model to validate the therapeutic effect of OMTX703. HSJD-ES-009 was considered the best candidate because of its relatively high ENG expression as well as its high rate of successful engraftment in mice as compared with the rest of the PDX models (Fig. 1G; Supplementary Fig. S9A and S9B). Irinotecan was used as reference drug because of its potent activity as single agent in preclinical models of pediatric solid tumors (Supplementary Table S10; ref. 21).

Criteria to quantify drug response are shown in Supplementary Table S11. Although animals did not experience weight loss during treatment (Fig. 6A), OMTX703 at 60 mg/kg produced an acute toxic death rate of 50%, with three animals dying at days 21, 22, and 28 from treatment initiation. Regarding this fact, we proceeded to thoroughly examine the drug-induced toxicity in FFPE samples of lung, liver, and kidney from the PDXs. However, by histopathological analyses, no significant differences were observed between the drug-treated and the control groups (Supplementary Tables S12–S14). Animals treated with OMTX003 experienced progressive tumor growth, as the control animals did. We found a dose-dependent antitumor response with OMTX703 at 30 and 60 mg/kg. Interestingly, OMTX703 at 60 mg/kg induced a complete response (CR) rate of 60% at day 21 of treatment, in comparison to the reference treatment (irinotecan) which induced CR in 11% of tumors (Fig. 6B and D).

To quantify the long-term effects of drug treatment upon survival, a second study was conducted. After cessation of treatments all groups experienced progressive tumor growth, with relapse occurring even in mice that had shown complete tumor response (Fig. 6C; Supplementary Fig. S9B). As with prior studies, no weight loss was observed during the survival study and weight gain was mainly due to the increase in tumor volume (Supplementary Fig. S9C). Median time to achieve endpoint is shown in Fig. 6E and F, with significant longer median time in OMTX703 (60 mg/kg) and irinotecan-treated animals as compared with control-treated mice [60 days, $P = 0.0065$ for OMTX703 (60 mg/kg); and 46 days, $P = 0.0018$ for irinotecan]. Finally, IHC was performed to evaluate the possible changes on ENG and MMP14 expression amongst groups (Supplementary Fig. S10A and S10B; Supplementary Tables S15 and S16) as well as proliferation rate by Ki67 staining (Supplementary Fig. S10C) and viability by H&E staining (Supplementary Fig. S9D). Compared with placebo-treated mice, we found a significant increase of ENG expression in mice treated with OMTX003 at 10 mg/kg ($P = 0.0005$; Supplementary Fig. S10A) and a significant increase of MMP14 expression in the groups treated with OMTX703 at 30 mg/kg ($P = 0.0316$), OMTX703 at 60 mg/kg ($P = 0.0163$), and irinotecan at 10 mg/kg ($P = 0.0240$) as reflected in Supplementary Fig. S10B.

Cell viability, measured by H&E, was not affected by the treatment in any case (Supplementary Fig. S9D). However, regarding the cell proliferation evaluated by Ki67 staining, we found a significant decrease in the group treated with OMTX003 10 mg/kg ($P = 0.0479$) and a nonsignificant decrease in the groups treated with OMTX703 (30 mg/kg; 60 mg/kg) and irinotecan 10 mg/kg (Supplementary Fig. S10C). From this result, we could hypothesize that cells with stable proliferation the ENG upregulation as a way to compensate its activity was impaired by the antibody blockade. MMP14 overexpression could be due to the strong blockade of cell proliferation, because this protein also plays an important role in cell cycle and proliferation.

Discussion

The present investigation is the first work to show the antitumor activity of ENG-targeting ADC therapies in Ewing sarcoma. We propose that this novel approach might provide improved tumor selectivity as compared with cytotoxic agents in a subset of patients with Ewing sarcoma expressing high levels of ENG. Most cytotoxic chemotherapies used today exhibit a narrow therapeutic index dependent upon a higher proliferative rate of tumor cells compared with normal cells. The implications of Ewing sarcoma heterogeneity in response to treatment also represent a challenge when it comes to defining upfront clinical strategies. These facts stress the need to selectively target the unique molecular features that exist in tumor cells while preventing off-target effects in normal cells. In this context, precision medicine represents an appealing yet rather challenging paradigm. Toward that end, ADCs have shown clinical promise given their ability to harness the specificity of monoclonal antibodies to more selectively deliver apoptosis-inducing molecules to epitope-bearing tumor cells (10, 22–24).

Although the pathognomonic hallmarks of Ewing sarcoma (i.e., the EWS–FLI1 fusion protein and CD99 overexpression) have been known for decades, only in the last years have Ewing sarcoma-specific trials taken direct aim at the oncogenic fusion protein or the ETS subcomponent (25). Although we eagerly await the clinical results from trials testing the first-generation EWS-FLI1 modulators, such as TK-216, the issue of innate and acquired intratumoral heterogeneity is likely to remain a significant hurdle that prevents—or at least substantially reduces—the likelihood that any single therapy will eradicate every tumor cell. Substantiating this concern, recent evidence from two laboratories suggests that Ewing sarcoma cells can oscillate between high- and low-expressing states with respect to the EWS–FLI1 fusion protein. Intriguingly, low levels of EWS–FLI1 might actually result in increased migration and invasion by tumor cells, questioning the effectiveness of exclusively targeting the ES fusion protein without cotargeting of other oncogenic drivers (5, 26). Although CD99 is highly expressed by Ewing sarcoma cells, MSCs and other cell types also express it in physiologic conditions (27). So far, no specific membrane receptors have been described for Ewing sarcoma, with the exception of LINGO1. Nonetheless, it was also expressed in the brain and its expression was highly variable in Ewing sarcoma when compared with that of CD99 (28).

The ENG receptor, as mentioned previously, is not tumor-specific and it is also expressed by normal vascular tissues. Mutations in ENG are associated with hereditary hemorrhagic telangiectasia type 1 (HHT1). HHT1 patients present massive vascular malformation (17). In cancer, the transmembrane form of ENG

Published OnlineFirst November 12, 2018; DOI: 10.1158/1078-0432.CCR-18-0936

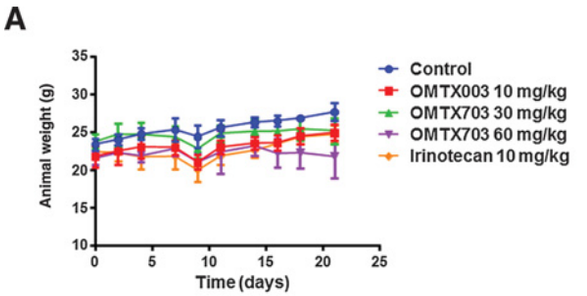

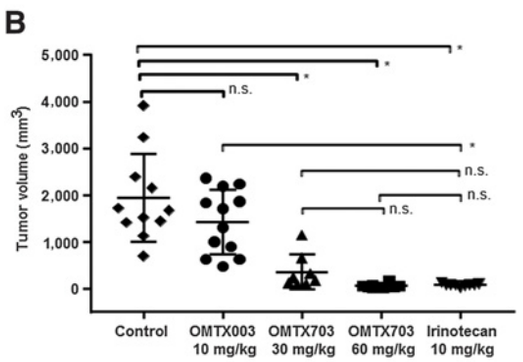

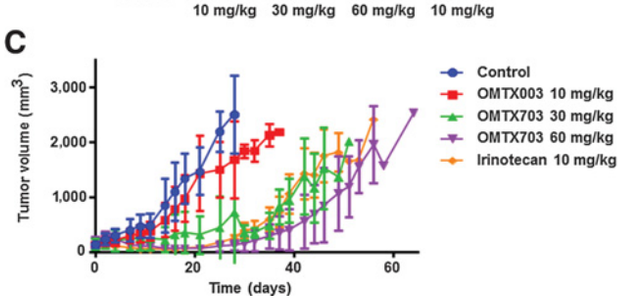

D

Treatment	*n*	PD (%)	SD (%)	PR (%)	CR (%)
Control	10	100	0	0	0
OMTX003 (10 mg/kg)	12	100	0	0	0
OMTX703 (60 mg/kg)	10	0	0	40	60
OMTX703 (30 mg/kg)	8	75	25	0	0
Irinotecan	9	11	55	22	11

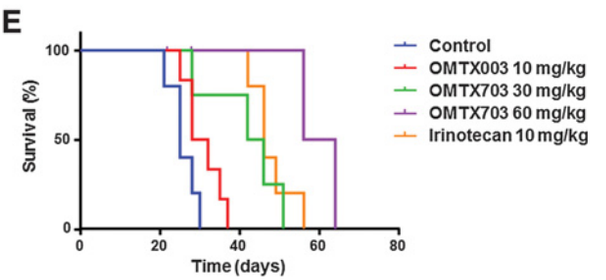

F

Treatment	*n*	MS (days)	*P* value
Control	5	25	--
OMTX003 10 mg/kg	6	30	0.0589
OMTX703 60 mg/kg	2	60	0.0065*
OMTX703 30 mg/kg	4	44	0.0220
Irinotecan	5	46	0.0018**

Figure 6.

OMTX703 leads to complete response and prolonged survival time in a Ewing sarcoma (ES) PDX model. We selected the PDX model with the highest expression of ENG as the best candidate to evaluate the efficacy of OMTX703. **A,** Body weights during OMTX003, OMTX703, and irinotecan treatments. No signs of toxicity in terms of weight loss were detected ($n = 6$ animals per group; means and SD). **B,** Tumor volumes at the end of treatment (21 days). Irinotecan-treated group was considered as the positive control of response ($n = 6$ animals per group; 8–12 tumors were evaluable in each group; individual tumor volumes are shown). *, $P < 0.0001$ (one way ANOVA with Tukey's multiple comparisons test); n.s., not significant. **C,** Efficacy study showing dose-dependent partial tumor growth inhibition with OMTX703. All mice showed progressive disease by the end of the study. **D,** Response at the end of treatment (day 21). PD, progressive disease; PR, partial response; SD, stable disease. **E,** Kaplan–Meier survival curves. **F,** Median survival (MS) times: the OMTX703-treated group presented the highest median survival (60 days) compared with the reference group treated with irinotecan (46 days). *, Significant as compared with control (log-rank test). Upon Bonferroni correction for multiple comparisons of the median survivals of treatment groups versus control group, *P* value threshold <0.0125 was considered significant.

has been associated with poor clinical outcomes, high intratumoral microvessel densities, and an aggressive/invasive phenotype in certain tumor types (18, 29, 30). Interestingly, the soluble form of ENG (sENG) has been described as an antagonist of transmembrane ENG and a biomarker of hypertension, diabetes, and preeclampsia (31, 32). sENG has also been pointed as a circulating biomarker of poor prognosis in patients with solid tumors (33, 34). However, our analysis of sENG in plasma showed no significant differences between healthy donors and patients with Ewing sarcoma, and no significant correlations with clinical parameters. To sum up, ENG presents two major roles in cancer biology: (i) modulating tumor angiogenesis and (ii) promoting tumor progression in certain tumor types; hence, it represents an attractive therapeutic target.

Previous works from other groups, hereby reproduced (Supplementary Fig. S4), have, in fact, shown that ENG-targeting with a humanized MAb impairs the ability of endothelial cells to form functional tubular structures, which are essential for tumor neoangiogenesis (11). ENG-targeting MAbs are currently being used in clinical trials for solid tumors, mainly in combination with other anti-angiogenic agents (35–37). Expression of ENG in Ewing sarcoma was previously described by our group in a small set of tumor samples (27). The role of ENG on Ewing sarcoma phenotype and malignancy has already been studied in *in vitro* and *in vivo* models, where ENG was associated with increased invasiveness and metastasis formation (18). In fact, ENG is described as a "gold" receptor protein in a recent work focused on the study of the *surfaceome* of Ewing sarcoma for the search of

targetable membrane receptors (28). Our finding of a possible epigenetic downregulation of ENG by methylation of its promoter region in the CADO cell line is consistent with other studies in solid tumors, where the hypermethylation of *ENG* promoter region results in gene silencing, and was reactivated after *in vitro* methylation reversal assays (38, 39). Moreover, the positive correlation between ENG and MMP14 observed in Ewing sarcoma cell lines and patients' samples, suggests that there might be an important highly regulated balance between both proteins.

A major strength of our work stems from the concurrent evaluation of ENG as a therapeutic target against Ewing sarcoma by two academic labs, based respectively in Europe and the United States, which focus on Ewing sarcoma drug development. As initial proof-of-concept, we evaluated OMTX503, a humanized MAb engaging ENG linked to a nontoxic type 2 ribosome-inactivating protein nigrin-b A chain, *in vitro* and within murine models. The development of an anti-ENG-nigrin-b-based ADC has already shown activity towards melanoma mouse tumors, both *in vitro* and *in vivo* (40). This work showed that targeting human ENG in a xenograft model with the ADC resulted in tumor shrinkage and inhibition of neo-angiogenesis (40). It is important to mention that this MAb engaging ENG is linked to the nontoxic A chain of nigrin-b.

Although OMTX503 demonstrated moderate preclinical activity, we subsequently transitioned our research focus to ENG-targeting ADC with cytolysin, OMTX703, given its lower toxicity and broader therapeutic window. OMTX503 and OMTX703 share the same mechanism of action and both lead to cell-death after drug internalization. Our *in vitro* results confirmed an ENG-dependent effect for both molecules. Ewing sarcoma cell line-derived xenografts with a high expression of ENG were used as a first *in vivo* approach. At this point, we found differences of response to treatment, depending on the drug administered, OMTX503 or OMTX703. We suggest that the response to treatment could be mainly influenced by the therapeutic window of each ADC.

Recognizing the potential importance of human tumor stroma in evaluating the anti-ENG ADC response, we sought to validate the xenograft results using Ewing sarcoma PDX models that likely exhibit a wider breadth of intratumoral heterogeneity that better reflects the clinical setting. Only OMTX703 was comprehensively assessed in PDXs. Notably, the frequency of CR (60%) after 21 days of treatment in PDXs treated with OMTX703 reinforces the promising efficacy of this drug. Given that all mice relapsed in the long-term survival study, we hereby suggest the importance of drug combinations to avoid acquired drug resistance.

Taken together, the antineoplastic effects observed in our Ewing sarcoma PDXs are highly encouraging. Although additional research is certainly required before one would propose using ENG expression in order to select patients receiving ENG-targeting therapies, the prospect of using ENG expression as a predictive biomarker of response would clearly represent a crucial step to identify patients with Ewing sarcoma most likely to benefit from anti-ENG ADC therapies and, additionally, enable tissue-based companion diagnostics. Similarly, the toxicity profiles associated to these molecules, need be to further analyzed in specific regulatory toxicologic studies in additional preclinical animal models. Although this study focused primarily on the direct effect of targeting ENG in tumor cells, future research must decipher how anti-ENG ADCs affect vascular stroma and the processes responsible for endothelial cell function and angiogenesis. In that regard, the capacity for OMTX703 to jointly target the tumor and stroma raises the tantalizing possibility that OMTX703 might delay tumor growth even when ENG expression is low or absent (36, 37). With the addition of more comprehensive toxicity data, ENG-targeting ADCs represent a promising therapeutic alternative that may someday help patients with ES suffering from ENG-positive tumors.

Disclosure of Potential Conflicts of Interest

R.E. Kontermann reports receiving commercial research grants from and is a consultant/advisory board member for Oncomatryx. K. Pfizenmaier reports receiving commercial research grants from and is a consultant/advisory board member for Oncomatryx. L. Simon is an employee of and holds ownership interest (including patents) in Permedika Entrepeneurs, Quimatryx, Sunrock Biopharma, Patia Biopharma, Nelum, Patia Europe, Stemtek Therapeutics, and Helenes Ventures. J.A. Ludwig is a consultant/advisory board member for Oncomatryx. E. de Álava reports receiving speakers bureau honoraria from Roche, Lilly, and Pfizer, and is a consultant/advisory board member for Roche. No potential conflicts of interest were disclosed by the other authors.

Authors' Contributions

Conception and design: P. Puerto-Camacho, A.T. Amaral, S.-E. Lamhamedi-Cherradi, S. Domínguez, K. Schadler, L. Simón, M. Fabre, Á.M. Carcaboso, J.A. Ludwig, E. de Álava

Development of methodology: P. Puerto-Camacho, A.T. Amaral, S.-E. Lamhamedi-Cherradi, B.A. Menegaz, J.L. Ordóñez, C. Jordan-Perez, J. Diaz-Martin, M. Lopez-Alvarez, K. Schadler, R. Kontermann, K. Pfizenmaier, J.A. Ludwig, E. de Álava

Acquisition of data (provided animals, acquired and managed patients, provided facilities, etc.): P. Puerto-Camacho, A.T. Amaral, S.-E. Lamhamedi-Cherradi, B.A. Menegaz, H. Castillo-Ecija, J.L. Ordóñez, C. Jordan-Perez, G. Civantos-Jubera, M.J. Robles-Frías, C. Ferrer, J. Mora, B. Cuglievan, Á.M. Carcaboso, J.A. Ludwig, E. de Álava

Analysis and interpretation of data (e.g., statistical analysis, biostatistics, computational analysis): P. Puerto-Camacho, A.T. Amaral, S.-E. Lamhamedi-Cherradi, B.A. Menegaz, H. Castillo-Ecija, J.L. Ordóñez, S. Domínguez, J. Diaz-Martin, L. Romero-Pérez, C. Ferrer, O. Seifert, M. Fabre, Á.M. Carcaboso, J.A. Ludwig, E. de Álava

Writing, review, and/or revision of the manuscript: P. Puerto-Camacho, A.T. Amaral, S.-E. Lamhamedi-Cherradi, B.A. Menegaz, S. Domínguez, J. Mora, O. Seifert, R. Kontermann, K. Pfizenmaier, M. Fabre, Á.M. Carcaboso, J.A. Ludwig, E. de Álava

Administrative, technical, or material support (i.e., reporting or organizing data, constructing databases): P. Puerto-Camacho, A.T. Amaral, S.-E. Lamhamedi-Cherradi, B.A. Menegaz, S. Domínguez, M. Biscuola, J. Mora, O. Seifert, R. Kontermann, K. Pfizenmaier, J.A. Ludwig

Study supervision: S.-E. Lamhamedi-Cherradi, S. Domínguez, L. Simón, Á.M. Carcaboso, J.A. Ludwig, E. de Álava

Acknowledgments

This research has been conducted using samples from the Hospital Universitario Virgen del Rocío - Instituto de Biomedicina de Sevilla Biobank (Andalusian Public Health System Biobank and ISCIII-Red de Biobancos PT13/0010/0056). The authors thank the donors and the Hospital Universitario Virgen del Rocío - Instituto de Biomedicina de Sevilla Biobank (Andalusian Public Health System Biobank and ISCIII-Red de Biobancos PT13/0010/0056) and Xarxa de Bancs de Tumors de Catalunya (XBTC) sponsored by Pla Director d'Oncologia de Catalunya for the human specimens used in this study. The authors thank Dr. Arjan Lankester, from LUMC, for providing the plasmas and clinical data from Ewing sarcoma patients.

The authors thank Drs. Ying Wang and Jing Wang from Bioinformatics and Computational Biology Department at MDACC for their contribution in performing the bioinformatic analyses regarding the RPPA profiling.

EDA's lab is supported by the RETOS COLABORACIÓN project (RTC-2014-2102-1); the AECC project (GCB13131578DEÁ); ISCIII-FEDER (PI14/

01466 and PI17/00464); CIBERONC (CB16/12/00361 and CB16/12/00316 Fundación CRIS contra el cáncer); and Asociación Pablo Ugarte. PPC is sponsored by the Fundación María García Estrada. AMC lab is supported by ISCIII-FEDER (CP13/00189). MJRF is supported by Consejería de Salud de la Junta de Andalucía (ECAIF2-0176-2013). J.A. Ludwig lab is supported by the NIH (R01 CA180279) and the University of Texas MD Anderson Cancer Center's Support Grant CA016672.

The costs of publication of this article were defrayed in part by the payment of page charges. This article must therefore be hereby marked *advertisement* in accordance with 18 U.S.C. Section 1734 solely to indicate this fact.

Received March 26, 2018; revised July 13, 2018; accepted November 6, 2018; published first November 12, 2018.

References

1. Biswas B, Bakhshi S. Management of Ewing sarcoma family of tumors: current scenario and unmet need. World J Orthop 2016;7:527–38.
2. Zucman J, Delattre O, Desmaze C, Plougastel B, Joubert I, Melot T, et al. Cloning and characterization of the Ewing's sarcoma and peripheral neuroepithelioma t(11;22) translocation breakpoints. Genes Chromosomes Cancer 1992;5:271–7.
3. Sheffield NC, Pierron G, Klughammer J, Datlinger P, Schonegger A, Schuster M, et al. DNA methylation heterogeneity defines a disease spectrum in Ewing sarcoma. Nat Med 2017;23:386–95.
4. Huertas-Martinez J, Court F, Rello-Varona S, Herrero-Martin D, Almacellas-Rabaiget O, Sainz-Jaspeado M, et al. DNA methylation profiling identifies PTRF/Cavin-1 as a novel tumor suppressor in Ewing sarcoma when co-expressed with caveolin-1. Cancer Lett 2017;386:196–207.
5. Franzetti GA, Laud-Duval K, van der Ent W, Brisac A, Irondelle M, Aubert S, et al. Cell-to-cell heterogeneity of EWSR1-FLI1 activity determines proliferation/migration choices in Ewing sarcoma cells. Oncogene 2017;36:3505–14.
6. Cornaz-Buros S, Riggi N, DeVito C, Sarre A, Letovanec I, Provero P, et al. Targeting cancer stem-like cells as an approach to defeating cellular heterogeneity in Ewing sarcoma. Cancer Res 2014;74:6610–22.
7. Schrama D, Reisfeld RA, Becker JC. Antibody targeted drugs as cancer therapeutics. Nat Rev Drug Discov 2006;5:147–59.
8. Citores L, Ferreras JM, Munoz R, Benitez J, Jimenez P, Girbes T. Targeting cancer cells with transferrin conjugates containing the non-toxic type 2 ribosome-inactivating proteins nigrin b or ebulin l. Cancer Lett 2002;184:29–35.
9. Munoz R, Arias Y, Ferreras JM, Rojo MA, Gayoso MJ, Nocito M, et al. Targeting a marker of the tumour neovasculature using a novel anti-human CD105-immunotoxin containing the non-toxic type 2 ribosome-inactivating protein nigrin b. Cancer Lett 2007;256:73–80.
10. Beck A, Goetsch L, Dumontet C, Corvaia N. Strategies and challenges for the next generation of antibody-drug conjugates. Nat Rev Drug Discov 2017;16:315–37.
11. Rosen LS, Gordon MS, Robert F, Matei DE. Endoglin for targeted cancer treatment. Curr Oncol Rep 2014;16:365.
12. Lastres P, Letamendia A, Zhang H, Rius C, Almendro N, Raab U, et al. Endoglin modulates cellular responses to TGF-beta 1. J Cell Biol 1996;133:1109–21.
13. Chen CZ, Li M, de Graaf D, Monti S, Gottgens B, Sanchez MJ, et al. Identification of endoglin as a functional marker that defines long-term repopulating hematopoietic stem cells. Proc Natl Acad Sci U S A 2002;99:15468–73.
14. Hawinkels LJ, Kuiper P, Wiercinska E, Verspaget HW, Liu Z, Pardali E, et al. Matrix metalloproteinase-14 (MT1-MMP)-mediated endoglin shedding inhibits tumor angiogenesis. Cancer Res 2010;70:4141–50.
15. Lopez-Novoa JM, Bernabeu C. The physiological role of endoglin in the cardiovascular system. Am J Physiol Heart Circ Physiol 2010;299:H959–74.
16. Arthur HM, Ure J, Smith AJ, Renforth G, Wilson DI, Torsney E, et al. Endoglin, an ancillary TGFbeta receptor, is required for extraembryonic angiogenesis and plays a key role in heart development. Dev Biol 2000;217:42–53.
17. McAllister KA, Grogg KM, Johnson DW, Gallione CJ, Baldwin MA, Jackson CE, et al. Endoglin, a TGF-beta binding protein of endothelial cells, is the gene for hereditary haemorrhagic telangiectasia type 1. Nat Genet 1994;8:345–51.
18. Pardali E, van der Schaft DW, Wiercinska E, Gorter A, Hogendoorn PC, Griffioen AW, et al. Critical role of endoglin in tumor cell plasticity of Ewing sarcoma and melanoma. Oncogene 2011;30:334–45.
19. van der Schaft DW, Hillen F, Pauwels P, Kirschmann DA, Castermans K, Egbrink MG, et al. Tumor cell plasticity in Ewing sarcoma, an alternative circulatory system stimulated by hypoxia. Cancer Res 2005;65:11520–8.
20. Hendrix MJ, Seftor EA, Hess AR, Seftor RE. Vasculogenic mimicry and tumour-cell plasticity: lessons from melanoma. Nat Rev Cancer 2003;3:411–21.
21. Stewart E, Goshorn R, Bradley C, Griffiths LM, Benavente C, Twarog NR, et al. Targeting the DNA repair pathway in Ewing sarcoma. Cell Rep 2014;9:829–41.
22. Krop IE, Kim SB, Gonzalez-Martin A, LoRusso PM, Ferrero JM, Smitt M, et al. Trastuzumab emtansine versus treatment of physician's choice for pretreated HER2-positive advanced breast cancer (TH3RESA): a randomised, open-label, phase 3 trial. Lancet Oncol 2014;15:689–99.
23. Gan HK, van den Bent M, Lassman AB, Reardon DA, Scott AM. Antibody-drug conjugates in glioblastoma therapy: the right drugs to the right cells. Nat Rev Clin Oncol 2017;14:695–707.
24. Lambert JM, Morris CQ. Antibody-drug conjugates (ADCs) for personalized treatment of solid tumors: a review. Adv Ther 2017;34:1015–35.
25. Ordonez JL, Osuna D, Herrero D, de Alava E, Madoz-Gurpide J. Advances in Ewing's sarcoma research: where are we now and what lies ahead? Cancer Res 2009;69:7140–50.
26. Barber-Rotenberg JS, Selvanathan SP, Kong Y, Erkizan HV, Snyder TM, Hong SP, et al. Single enantiomer of YK-4-279 demonstrates specificity in targeting the oncogene EWS-FLI1. Oncotarget 2012;3:172–82.
27. Amaral AT, Manara MC, Berghuis D, Ordonez JL, Biscuola M, Lopez-Garcia MA, et al. Characterization of human mesenchymal stem cells from Ewing sarcoma patients. Pathogenetic implications. PLoS One 2014;9:e85814.
28. Town J, Pais H, Harrison S, Stead LF, Bataille C, Bunjobpol W, et al. Exploring the surfaceome of Ewing sarcoma identifies a new and unique therapeutic target. Proc Natl Acad Sci U S A 2016;113:3603–8.
29. Dallas NA, Samuel S, Xia L, Fan F, Gray MJ, Lim SJ, et al. Endoglin (CD105): a marker of tumor vasculature and potential target for therapy. Clin Cancer Res 2008;14:1931–7.
30. Uneda S, Toi H, Tsujie T, Tsujie M, Harada N, Tsai H, et al. Anti-endoglin monoclonal antibodies are effective for suppressing metastasis and the primary tumors by targeting tumor vasculature. Int J Cancer 2009;125:1446–53.
31. Blazquez-Medela AM, Garcia-Ortiz L, Gomez-Marcos MA, Recio-Rodriguez JI, Sanchez-Rodriguez A, Lopez-Novoa JM, et al. Increased plasma soluble endoglin levels as an indicator of cardiovascular alterations in hypertensive and diabetic patients. BMC Med 2010;8:86.
32. Young BC, Levine RJ, Karumanchi SA. Pathogenesis of preeclampsia. Annu Rev Pathol 2010;5:173–92.
33. Takahashi N, Kawanishi-Tabata R, Haba A, Tabata M, Haruta Y, Tsai H, et al. Association of serum endoglin with metastasis in patients with colorectal, breast, and other solid tumors, and suppressive effect of chemotherapy on the serum endoglin. Clin Cancer Res 2001;7:524–32.
34. Vo MN, Evans M, Leitzel K, Ali SM, Wilson M, Demers L, et al. Elevated plasma endoglin (CD105) predicts decreased response and survival in a metastatic breast cancer trial of hormone therapy. Breast Cancer Res Treat 2010;119:767–71.
35. Rosen LS, Hurwitz HI, Wong MK, Goldman J, Mendelson DS, Figg WD, et al. A phase I first-in-human study of TRC105 (anti-endoglin antibody) in patients with advanced cancer. Clin Cancer Res 2012;18:4820–9.
36. Gordon MS, Robert F, Matei D, Mendelson DS, Goldman JW, Chiorean EG, et al. An open-label phase Ib dose-escalation study of TRC105 (anti-

endoglin antibody) with bevacizumab in patients with advanced cancer. Clin Cancer Res 2014;20:5918–26.
37. Liu Y, Tian H, Blobe GC, Theuer CP, Hurwitz HI, Nixon AB. Effects of the combination of TRC105 and bevacizumab on endothelial cell biology. Invest New Drugs 2014;32:851–9.
38. O'Leary K, Shia A, Cavicchioli F, Haley V, Comino A, Merlano M, et al. Identification of endoglin as an epigenetically regulated tumour-suppressor gene in lung cancer. Br J Cancer 2015;113:970–8.
39. Wong VC, Chan PL, Bernabeu C, Law S, Wang LD, Li JL, et al. Identification of an invasion and tumor-suppressing gene, endoglin (ENG), silenced by both epigenetic inactivation and allelic loss in esophageal squamous cell carcinoma. Int J Cancer 2008;123:2816–23.
40. Munoz R, Arias Y, Ferreras JM, Jimenez P, Langa C, Rojo MA, et al. In vitro and in vivo effects of an anti-mouse endoglin (CD105)-immunotoxin on the early stages of mouse B16MEL4A5 melanoma tumours. Cancer Immunol Immunother 2013;62:541–51.

Published OnlineFirst November 12, 2018; DOI: 10.1158/1078-0432.CCR-18-0936

Clinical Cancer Research

Preclinical Efficacy of Endoglin-Targeting Antibody–Drug Conjugates for the Treatment of Ewing Sarcoma

Pilar Puerto-Camacho, Ana Teresa Amaral, Salah-Eddine Lamhamedi-Cherradi, et al.

Clin Cancer Res 2019;25:2228-2240. Published OnlineFirst November 12, 2018.